Science of the Total Environment 826 (2022) 154111

Contents lists available at ScienceDirect

Science of the Total Environment

journal homepage: www.elsevier.com/locate/scitotenv

The potential of groundwater-dependent ecosystems to enhance soil biological activity and soil fertility in drylands

M. Trinidad Torres-García [a,b,*], Cecilio Oyonarte [b,c], Javier Cabello [a,b], Emilio Guirado [b,d], Borja Rodríguez-Lozano [c], M. Jacoba Salinas-Bonillo [a,b]

[a] Department of Biology and Geology, University of Almería, Spain
[b] Andalusian Centre for the Monitoring and Assessment of Global Change (CAESCG), University of Almería, Almería, Spain
[c] Department of Agronomy, University of Almería, Almería, Spain
[d] Instituto Multidisciplinar para el Estudio del Medio "Ramón Margalef", University of Alicante, Alicante, Spain

HIGHLIGHTS

- Groundwater connection enhances soil fertility in vegetation patches.
- Soil respiration responded to precipitation pulses more intensively under the patches.
- Phreatophytes foster fertile islands, enhancing mineralization rates and soil quality.
- Fertile islands are key for preserving the functional diversity of dryland ecosystems.

GRAPHICAL ABSTRACT

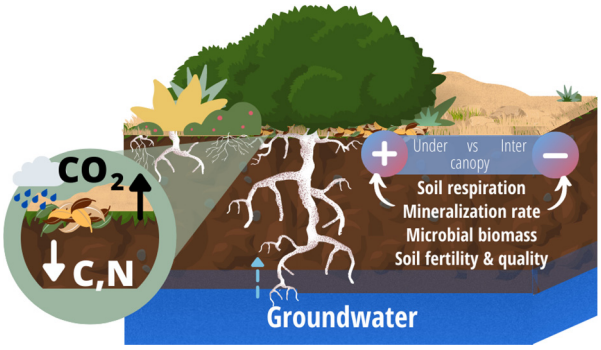

ARTICLE INFO

Article history:
Received 25 October 2021
Received in revised form 28 January 2022
Accepted 20 February 2022
Available online 24 February 2022

Editor: Jose Julio Ortega-Calvo

Keywords:
Fertility island
Normalized difference vegetation index (NDVI)
Soil microbial biomass
Semi-arid region
Soil quality
Ziziphus lotus

ABSTRACT

Water availability controls the functioning of dryland ecosystems, driving a patchy vegetation distribution, unequal nutrient availability, soil respiration in pulses, and limited productivity. Groundwater-dependent ecosystems (GDEs) are acknowledged to be decoupled from precipitation, since their vegetation relies on groundwater sources. Despite their relevance to enhance productivity in drylands, our understanding of how different components of GDEs interconnect (i.e., soil, vegetation, water) remains limited. We studied the GDE dominated by the deep-rooted phreatophyte *Ziziphus lotus*, a winter-deciduous shrub adapted to arid conditions along the Mediterranean basin. We aimed to disentangle whether the groundwater connection established by *Z. lotus* will foster soil biological activity and therefore soil fertility in drylands. We assessed (1) soil and vegetation dynamics over seasons (soil CO_2 efflux and plant activity), (2) the effect of the patchy distribution on soil quality (properties and nutrient availability), and soil biological activity (microbial biomass and mineralization rates) as essential elements of biogeochemical cycles, and (3) the implications for preserving GDEs and their biogeochemical processes under climate change effects. We found that soil and vegetation dynamics respond to water availability. Whereas soil biological activity promptly responded to precipitation events, vegetation functioning relies on less superficial water and responded on different time scales. Soil quality was higher under the vegetation patches, as was soil biological activity. Our findings highlight the importance of groundwater connections and phreatophytic vegetation to increase litter inputs and organic matter into the soils, which in turn enhances soil quality and decomposition processes in drylands. However, biogeochemical processes are jeopardized in GDEs by climate change effects and land degradation due to the dependence of soil activity on:

* Corresponding author at: University of Almería, Carretera de Sacramento s.n, La Cañada de San Urbano, Almería 04120, Spain.
E-mail address: m.t.torres@ual.es (M.T. Torres-García).

http://dx.doi.org/10.1016/j.scitotenv.2022.154111

(1) precipitation for activation, and (2) phreatophytic vegetation for substrate accumulation. Therefore, desertification might modify biogeochemical cycles by disrupting key ecosystem processes such as soil microbial activity, organic matter mineralization, and plant productivity.

1. Introduction

Arid and semiarid regions, covering 41% of Earth's land surface (Reynolds et al., 2007), are characterized by less annual precipitation than potential evapotranspiration, leading to prolonged dry periods (Newman et al., 2006). Since water shortage limits biological activity, their ecosystems are considered to be of low productivity (Noy-Meir, 1973; Tucker and Reed, 2016), because their primary production is partially controlled by precipitation events (Austin et al., 2004). Global-scale studies have shown the increasing importance of dryland ecosystems and their carbon stocks in the global carbon cycle (Poulter et al., 2014). However, our understanding of the spatiotemporal connections of the different ecosystem components remains limited.

Climate controls on biogeochemical cycles are critical in arid and semiarid regions where biological activity mainly depends on water availability (Delgado-Baquerizo et al., 2013). The presence of water after long dry periods usually triggers a cascade of physical, chemical, and biological processes (Potts et al., 2008) that depend on the magnitude and frequency of the precipitation event (Austin et al., 2004). Overall, precipitation events occurring in the dry season increase aboveground net primary productivity because of the alleviation of drought stress (Thomey et al., 2011). Higher water availability after a drought period also promotes the immediate net carbon release by enhancing soil respiration (Rs) (Birch effect; Birch, 1959) that encompasses both the autotrophic respiration of plant roots and rhizosphere activity, and the heterotrophic respiration of microbial communities (Oyonarte et al., 2012; Schlesinger and Andrews, 2000). The effect of precipitation on Rs and soil carbon stocks will depend on the distribution of available resources and soil microorganisms (Austin et al., 2004).

The study of carbon fluxes in dryland ecosystems is particularly challenging due to the marked seasonality of precipitation and high spatial heterogeneity of vegetation, nutrients, and resources. The spatial distribution of the vegetation in patches (Aguiar and Sala, 1999) leads to unequal distribution of nutrients and water and thus, to the development of 'islands of resources' or 'fertile islands' surrounded by relatively infertile soils (Reynolds et al., 1999). Shrub-dominated vegetation promotes sediment and nutrient accumulation under the canopy (Wang et al., 2019; Zhang et al., 2011). These accumulations can form structures called *nebkhas*, which are mainly observed in desert or coastal areas with patchy vegetation and high wind activity (Lang et al., 2013; Zhang et al., 2011).The heterogeneity of these ecosystems contributes to the spatial variability of carbon and nitrogen pools (Austin et al., 2004).

The abundance, diversity, and composition of soil microbial communities regulate key ecosystem processes in drylands, such as litter decomposition and organic matter mineralization (Delgado-Baquerizo et al., 2016; Ochoa-Hueso et al., 2018). Microbial activity releases C and nutrients from soil organic matter (SOM), which are essential for plant nutrient availability (Lambers and Oliveira, 2019). Larger amounts of litter and organic matter accumulated under the plant canopy promotes higher decomposition rates by microbial activity (Gallardo and Schlesinger, 1992). In contrast, bare soils accumulate less SOM, and its mineralization is mainly driven by abiotic factors such as solar radiation (i.e., photodegradation), particularly in drylands during summer (Rey et al., 2011). Thus, dryland ecosystems can also show significant heterogeneity in the degradation and mineralization processes driven by the spatial distribution of the vegetation in fertile islands and the climatic conditions.

Terrestrial groundwater-dependent ecosystems (GDEs) are constituted by phreatophytic vegetation that access to the groundwater via the capillary fringe (i.e., the unsaturated zone above the water table) and the development of deep root systems (Eamus et al., 2006; Glenn et al., 2013). GDEs represent a distinctive type of ecosystem in drylands where water limitation is mitigated. The functioning of the entire ecosystem is often inferred from phreatophytes and therefore, the ecosystem productivity is considered to be decoupled from precipitation (Eamus et al., 2006; Sommer and Froend, 2011). Notwithstanding, soil moisture, and thus precipitation, is a key factor controlling biological processes in drylands (Noy-Meir, 1973) such as soil microbial activity, which in turn influence soil fertility and nutrient availability (Delgado-Baquerizo et al., 2013; Querejeta et al., 2021; Sponseller, 2007). GDEs maintain critical functions in drylands since phreatophytes have more available water to sustain photosynthesis, and therefore to grow for longer periods than other dryland ecosystems.

The groundwater reliance of GDEs means that variations in groundwater availability would significantly alter the structure and function of the ecosystem, and even degrade it irreversibly (Colvin et al., 2003; Eamus et al., 2006). Climate change effects in drylands, which include decreases in water availability, more irregular and intense rainfall events, and prolonged droughts (Guiot and Cramer, 2016), are likely to reduce infiltration and thus groundwater recharge (Eamus et al., 2006), altering water and biogeochemical cycles. Added to the increase in transpiration by phreatophytes because of higher evapotranspirative demand (Nichols, 1994), climate change can produce a synergistic effect that would increase aquifer discharge and deplete the water table (Eamus et al., 2006). Water table declines could diminish the ecophysiological functioning of phreatophytes, and even cause extensive mortality when the root growth rate is exceeded (Orellana et al., 2012). Consequently, essential ecosystem functions such as primary production and microbial mineralization will be affected (Delgado-Baquerizo et al., 2013; Querejeta et al., 2021).

Recent studies have focused on defining the relationship of phreatophytes with groundwater (Antunes et al., 2018; Torres-García et al., 2021b; Zolfaghar et al., 2014), or with nutrient acquisition (Querejeta et al., 2021), whereas the interconnection with essential processes occurring in the soil, such as soil respiration or mineralization, are less studied in GDEs. Moreover, the potential for groundwater connection to enhance soil fertility and soil quality in drylands is overlooked. Here, we focus on the GDE dominated by the long-lived, winter-deciduous phreatophyte *Ziziphus lotus* (L.) Lam. (*Rhamnaceae*) in a semiarid region in the southwestern continental Europe. As *Z. lotus* is a facultative phreatophyte and the keystone species that dominates the GDE, the ecosystem functioning is partially decoupled from precipitation (Torres-García et al., 2021b) when groundwater connection is maintained. Nevertheless, the marked seasonality and scarcity of precipitation, and the high spatial heterogeneity of vegetation in arid and semiarid ecosystems can promote different responses in soil and vegetation activity.

Because soil biological activity in drylands is strongly tied to precipitation events (Austin et al., 2004; Rey et al., 2011; Rey et al., 2021; Vargas et al., 2018), but also to litter and organic matter inputs (Gallardo and Schlesinger, 1992), we hypothesize that the groundwater connection established by the phreatophyte *Z. lotus* will foster soil biological activity and therefore soil fertility under vegetation canopy. However, precipitation and thus, soil humidity in the topsoil layers might still be essential for activating soil processes, allowing plant nutrient acquisition in this arid GDE. Therefore, we aimed to assess (1) the dynamics of soil respiration (Rs) and vegetation over the seasons, (2) the effect of the vegetation patches on soil biological activity and soil quality (properties and nutrient availability) by comparing under canopy and inter-canopy scenarios, and (3) the implications for preserving arid GDEs and their biogeochemical processes under climate change effects.

2. Materials and methods

2.1. Site description

The study was conducted in a semiarid shrubland in the coastal plain of Cabo de Gata-Níjar Natural Park, Southeast of Spain (36.830606,

−2.293612), where the phreatophyte *Ziziphus lotus* is the keystone species of the protected European Habitat '*arborescent matorral with Ziziphus*' (Habitat 5220*, 92/43/CEE) (Fig. 1). The area is crossed by an intermittent stream, which seldom overflows, and is located over a coastal detritic aquifer, which comprises Plio-Pleistocene conglomerates with aeolian sands and Pliocene marine marls (Vallejos et al., 2018). The climate is characterized as Mediterranean and semiarid, with hot, dry summers, mild winters and mean annual temperature of 18 °C (Machado et al., 2011). During summer (mostly July and August), scarcely any precipitation event occurs in the area (Fig. S1). The mean annual precipitation of 220 mm is unevenly distributed during spring and autumn, although with intense and short recurrent events (i.e., precipitation pulses) in the late summer.

Groundwater depth, considered from the topographic surface to the water table, ranges from 2.1 m to 25.4 m, with slight increases from spring to summer (Torres-García et al., 2021a). Daily fluctuations in groundwater depth (0.08 cm) and even periodical variability because of the tides (more than 15 cm in 10 days) are commonly observed near the coast, whereas seasonal ones are more noticeable at the inner parts of the plain (groundwater reductions up to 18 cm from spring to summer) (Torres-García et al., 2021a).

Z. lotus is a winter-deciduous shrub very well adapted to semiarid and arid conditions due to its deep root system, which can reach up to 60 m (Le Houérou, 2006), and groundwater dependency (Guirado et al., 2018), which confer the ability to thrive during summer in our study area (Torres-García et al., 2021b). *Z. lotus* can be found in vast territories in North Africa and the Middle East, and it is sparsely present in south Europe, particularly in southeast Spain, Sicily, and Cyprus (Sánchez-Gómez et al., 2003; Guirado et al., 2017). Its individuals, with hemispherical shape (up to 4 m tall and 200 m^2 area; Guirado et al., 2019) and a thorny intricate architecture constitute vegetation patches with less sizable, Mediterranean shrubs such as *Salsola oppositifolia* Desf., *Lycium intricatum* Boiss., *Withania frutescens* (L.) Pauquy, and *Asparagus albus* L. These non-phreatophytic species distribute their rooting system within the first 0.9 m of the soil (De Baets et al., 2007). The vegetation shows a dispersed pattern with a patchy distribution typical of arid and semiarid regions (Tirado, 2009). *Z. lotus* is photosynthetically active during spring and summer (leaf flushing occurs in March and abscission from September, Torres-García et al., 2021c), whereas the rest of the plant species grow in winter. Litter is accumulated beneath the *Z. lotus* canopy whereas the rest of the soil surface is mostly bare or with sparse, tiny, annual plants.

Beneath the canopy the soil is deeper (albic Arenosols, more than 50 cm) with different horizons (Ah, Bw, C), whereas the space between plants shows shallow soils (calcaric Leptosols, c.a. 20 cm) without soil horizonation (Ah, Cmk). Both typologies show a sandy texture (>90% of sand), low water retention capacity, and alkaline pH.

2.2. Experimental design and sampling

We selected four patches of vegetation along the study coastal plain with groundwater availability that ranged between 7 and 19 m depth, but with minimum temporal variations in the water table (neither tides effect or significant seasonal variability). Each patch, which consisted of a mature individual of *Z. lotus* (>10 m^2) surrounded by small shrubs (<5% of total patch area), needed to be upright enough to get inside it. For each patch we selected three sites under the canopy (hereafter: under-canopy) and three surrounding sites with bare soil (inter-canopy), 2 to 4 m apart from vegetation (Fig. 1). At each site, we placed polyvinyl chloride (PVC) collars to monitor Rs dynamics and collected three soil subsamples from the first 10 cm of the topsoil around each collar to obtain a composite sample (Fig. S2). Sampling was conducted in August 2019 just before the late-summer rainfall. Composite samples were air-dried at 25 °C approximately, sieved to 2 mm (fine-earth fraction) to remove litter and coarse gravels, and then divided and stored at 4 °C in two subsets, one for mineralization experiments and other for soil property analysis.

2.3. In situ soil respiration measurements

To obtain monthly discrete measurement of CO_2 effluxes from April of 2018 to April 2019, we used a manual and portable opaque soil chamber system (EGM-4, PP-systems, Hitchin, UK). The chamber was located over the PVC collars (15 cm in diameter and 7 cm in height) that were inserted 3.5 cm into the soil and placed around the four selected patches to obtain soil respiration measurements, both under-canopy and inter-canopy (Fig. 1). The 24 collars remained undisturbed until the end of the

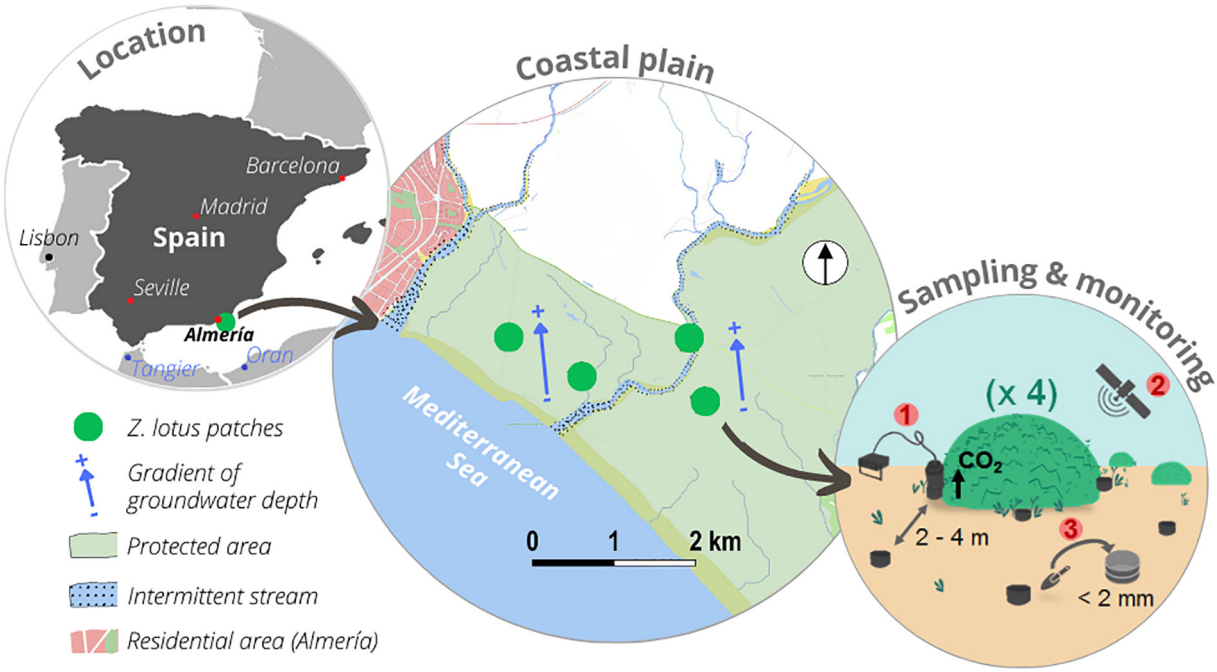

Fig. 1. Study area. Location, distribution of *Ziziphus lotus* patches in the coastal plain, and experimental design of the study in patches of *Z. lotus*. Bottom right circle summarizes the methodological sections of sampling and monitoring including: 1) in situ soil respiration monitoring, 2) remote sensing monitoring, and 3) soil sampling for mineralization and soil properties analyses.

experiment. Small grasses, litter, and insects were carefully removed from each collar before measuring. Because of the low CO_2 efflux rates, each collar was monitored for 120 s and measurements were recorded every 4 s to ensure reliable data. CO_2 efflux was estimated from the slopes of the CO_2 molar fractions of the confined air versus time (Pérez-Priego et al., 2010). To explain soil activity, soil temperature and soil volumetric water content (SWC) were measured at 5 cm depth with a digital thermometer and a portable theta probe (ML2x, Devices Ltd., Cambridge, UK) respectively, next to each collar and at the time of Rs measurement. All measurements were completed between 11:00 and 13:00 to avoid strong diurnal fluctuations, and in random order each time to avoid biased estimates.

2.4. Vegetation functioning from remote sensing monitoring

To assess vegetation dynamics and soil activity during a year in the GDE, we compared the seasonal dynamics of the normalized difference vegetation index (NDVI; Rouse et al., 1974) above and outside *Z. lotus*-dominated patches.

NDVI derived from satellite imagery (e.g. Landsat 30 m/pixel, MODIS/Terra 250 m/pixel), is widely used as a proxy for net primary productivity (Paruelo et al., 1997; Tian et al., 2017) and is calculated:

$$NDVI = \frac{R_{NIR} - R_{RED}}{R_{NIR} + R_{RED}} \quad (1)$$

where R_{NIR} is the reflectance of the near infrared band and R_{RED} is the reflectance of the red band. In this case, due to the size of *Z. lotus* shrubs (ca. 30 m^2; Guirado et al., 2017; Guirado et al., 2019) we used images provided by Cubesats from Planet (https://www.planet.com/) with a spatial resolution of 3 m/pixel and a spectral resolution in 4 bands: red (590–670 nm), green (500–590 nm), blue (455–515 nm), and NIR (780–860 nm).

We adjusted the monthly NDVI calculation (Eq. (1)) above *Z. lotus* (i.e. from 4 to 16 cloud-free pixels per sample within the patch) and outside these patches measuring 36 m^2 (4 pixels per sample). The study period was from April 2018 to April 2019. For that period, we also obtained daily meteorological data (precipitation and temperature from the Spanish Meteorological Agency) to explain vegetation dynamics.

2.5. Soil mineralization experiments

Bringing the soils into the laboratory allow us to remove the autotrophic component and water limitation, and the carbon fluxes obtained can therefore be attributed to carbon substrate, microbial biomass, and mineralization rates (Butterly et al., 2009; Gallardo and Schlesinger, 1992). First, we used the soil-induced respiration method (SIR) to assess microbial biomass carbon (C_{mic}) in real time, as described in Anderson and Domsch (1978). Briefly, under-canopy and inter-canopy soil samples (12 samples each × 3 replicates) were pre-incubated for 24 h in glass jars at 25 °C, after adding water (Fig. S3). Subsequently, a glucose solution was added to stimulate respiration and remove substrate limitation. The glass jars that contained the soil samples were immediately sealed with plastic gas-tight lids that had septum ports with rubber septa. Samples were incubated for 6 h with control conditions of humidity (60% of soil water holding capacity) and temperature (25 °C). A 0.5 ml volume of air was captured from the sealed jars to assess CO_2 concentration using an infrared CO_2 Analyser (Q-box SR1LP Soil respiration package, Qubit Systems, Canada). C_{mic} was then estimated according to the recalibration of West and Sparling (1986) at 25 °C (Eq. (2)) from the original equation of Anderson and Domsch (1978):

$$C_{mic} = 32.8 * [CO_2] + 3.7 \quad (2)$$

where C_{mic} is expressed in $\mu g\ g^{-1}$ soil, and $[CO_2]$ refers to the concentration of CO_2 ($\mu l\ CO_2\ g^{-1} soil\ h^{-1}$).

Second, we evaluated soil mineralization dynamics. In this case, the dry soil samples were pre-incubated for 24 h at 25 °C. Water was then added, the samples were sealed, and the first measurement was obtained 1 h afterwards to capture the initial pulse of CO_2. The same conditions of humidity (60% of soil water holding capacity) and temperature (25 °C) were maintained throughout the experiment. A volume of 0.5 ml of air was obtained from the sealed jars and CO_2 concentration was immediately measured with the infrared CO_2 analyser. After each measurement, the jars with the samples were opened to refresh the headspace with the room air and immediately sealed until the next day. We continued measuring CO_2 concentration every 24 h for 23 days, when measures stabilized.

2.6. Soil properties analyses

Two carbon fractions were analysed: (1) total organic carbon content (TOC) and (2) water extractable organic carbon (WEOC). TOC was determined by the Walkley–Black dichromate oxidation procedure modified by Mingorance et al. (2007) using a UV-spectrophotometer. WEOC was extracted following the procedure described in Embacher et al. (2007). Briefly, 25 g of soil sample was shaken for 30 min with 10 mM $CaCl_2$ with a soil:solvent ratio of 1:2 (w/w). The solution was centrifuged for 15 min at 6000 rpm to accelerate the subsequent filtration. The solution was then desiccated, and the carbon content estimated from the residue using the same method as for TOC (Mingorance et al., 2007).

Total nitrogen (N_{tot}) was determined by elemental analysis with a Leco TruSpec CN analyser, using fine soil samples. The carbon/nitrogen ratio was obtained from this variable and TOC.

The main components in the soil solution (nitrite, nitrate, phosphate, and sulphate) were also estimated using the liquid extraction method in a 1:5 soil/water solution (10 g soil: 50 ml water). Once the soil solution was obtained, anions were measured by liquid chromatography with a PHOTOSTORE chromatograph, Chromeleon model, using a standard curve with a mixture of anions at concentrations of 0, 5, 10, 15 and 30 ppm.

2.7. Statistical analysis

A linear mixed-effects model was used to analyse the spatial (cover: under-canopy vs. inter-canopy) and temporal (time: month) effects, as well as the interaction of both factors, on soil carbon fluxes (CO_2 efflux), soil water content (SWC), and soil temperature separately. Canopy, time, and their interaction were established as fixed effects of the model, whereas individual plants and collars nested to the canopy conditions were random effects. The best fitting model was selected based on restricted maximum likelihood (REML) values. We also applied a linear model to detect relationships between CO_2 efflux, SWC and soil temperature at 0–5 cm depth. To detect temporal variations in the dynamic of vegetation (NDVI), a two-way analysis of variance (ANOVA) was applied.

To identify spatial differences in C_{mic}, mineralization rate and soil properties (soil-nutrient availability and carbon fractions) we used a one-way ANOVA. We also used an analysis of covariance (ANCOVA) to compare the relationship between mineralization rates and soil carbon under- and inter-canopy. All analyses were performed in R with the functions *lmer* from the 'lme4' package, and *lm* and *aov* from the 'stats' package (version 3.5.2, R Core Team, 2018).

3. Results

3.1. Soil and vegetation dynamics

Our results revealed significant spatio-temporal differences in soil temperature, soil water content, CO_2 effluxes, and vegetation activity (Table 1, Table S1, and Fig. 2). Mean soil temperature was significantly higher inter-canopy than under-canopy, ranging from 14 °C to 37 °C (Fig. 2a). In spring and particularly in summer, we observed higher temperatures but also wider differences between canopies, whereas such differences and general mean soil temperature decreased in autumn and winter, reaching a minimum in December (14.2 ± 0.5 °C and 15.7 ± 0.7 °C under- and inter-canopy respectively). Likewise, mean soil water content (SWC) was

Table 1
Mean values (±SE) of soil environmental conditions (temperature and water content, SWC), CO_2 efflux, and normalized difference vegetation index (NDVI) for the period 2018/2019, differentiating between under- and inter-canopy. *F*-statistic and significance of the analysis are shown (***$P < 0.001$).

	Under-canopy	Inter-canopy	*F*	Significance
Soil Temp. (°C)	22.62 ± 0.65	26.49 ± 0.73	13.71	***
SWC (%)	3.63 ± 0.19	4.88 ± 0.19	77.68	***
CO_2 efflux (μmol CO_2 m^{-2} s^{-1})	1.02 ± 0.10	0.58 ± 0.02	48.27	***
NDVI[a]	0.23 ± 0.01	0.08 ± 0.01	168.8	***

[a] Differences between canopy and inter-canopy.

significantly higher inter-canopy (Table 1), although no seasonal dynamic was noticed (Fig. 2b). It was just in the single measurements of October and April when maximum values were recorded. Precipitation events were also more intense and frequent during these periods (early autumn and spring, Fig. 2e, Fig. S1).

Conversely, mean CO_2 efflux was 1.8 times greater under-canopy than inter-canopy (Table 1). Maximum mean rates occurred under-canopy in October 2018 (2.44 ± 0.13 μmol CO_2 m^{-2} s^{-1}) and April 2019 (3.62 ± 0.43 μmol CO_2 m^{-2} s^{-1}), whereas minimum one was measured in March inter-canopy (0.31 ± 0.04 μmol CO_2 m^{-2} s^{-1}) (Fig. 2c). The linear model revealed that both soil temperature and water content affected CO_2 efflux ($F = 22.49$, $P < 0.001$, $R^2 = 0.22$), although with a more significant influence of the latter ($P < 0.001$) than the former ($P = 0.002$).

When analysing vegetation activity (measured as NDVI), we observed significant differences between canopy and inter-canopy (Table 1). NDVI for the vegetated areas followed a seasonal pattern with bimodal maximums (June and December) associated with the green-leaf periods of phreatophyte and non-phreatophyte species respectively (Fig. 2d,f). Minimum values were observed in September and March, which coincided with the end of senescence periods. Whereas the vegetation activity increased in spring with the rise of soil temperature and precipitation, the inter-canopy signal showed a decrease from May to August. Later in autumn, when precipitation period began, both NDVI curves rise. Therefore, not only does soil biological activity respond to SWC, but also vegetation dynamics to higher water availability, albeit with different time lags.

3.2. Soil microbial biomass and mineralization rates

The incubation experiments revealed higher levels of soil microbial biomass (C_{mic}) and mineralization rates under-canopy than inter-canopy (Table 2) when removing water limitation. C_{mic} was twice as high under-canopy (7.51 ± 0.13 mg kg^{-1} soil) as inter-canopy (3.90 ± 0.02 mg kg^{-1} soil), whereas the magnitude of soil mineralization rate was approximately 16 times higher under-canopy (Table 2). Soil mineralization experienced a rapid decrease during the first 24 h of incubation, both under- and inter-canopy (from Day 1 to Day 2; Fig. 3). We observed clear differences between mineralization curves with higher rates and more complex dynamics under-canopy, and lower and constant rates inter-canopy. The steep decline continued up to Day 10 under-canopy, although with higher CO_2 concentrations on Day 6 and Day 8. We also recorded a peak on Day 6 inter-canopy. From Day 10, minor fluctuations were observed at both sites. The differences between the mineralization under- and inter-canopy increased with time, reaching maximums on Day 8 and 17 (rates of 36 and 29 times higher under-canopy, respectively).

3.3. Soil properties and fertility

In general, we observed higher concentrations of carbon and nutrients under-canopy than inter-canopy (Table 3). Both total organic carbon (TOC) and the extractable fraction (WEOC) were significantly higher under-canopy ($P < 0.001$). Regarding nitrogen, higher concentrations

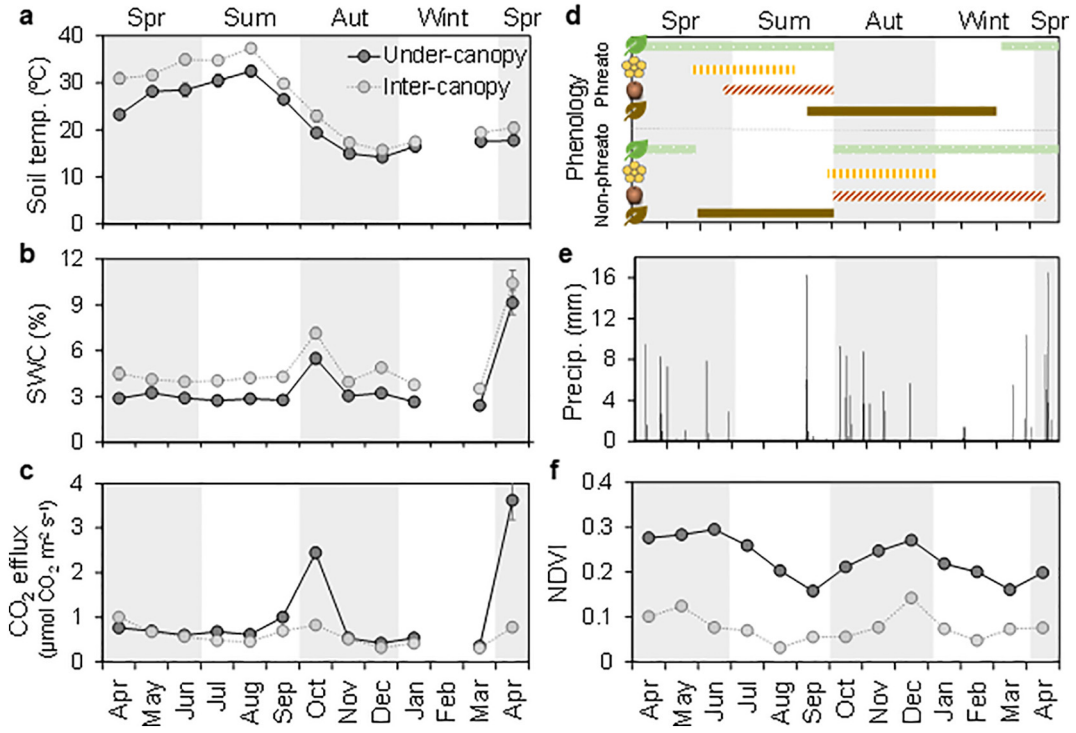

Fig. 2. Dynamics of variables related to soil (left panels) and vegetation (right panels) functioning from April 2018 to April 2019. Mean values (±SE) under-canopy (dark circles) and inter-canopy (light ones) of (a) soil temperature, (b) soil water content (SWC) and (c) CO_2 efflux. Note that no measurements were obtained in February 2019. d) Phenology of phreatophyte (*Z. lotus* from Torres-García et al., 2021c) and non-phreatophyte species present in the study area (Martín and Escarré, 1980): Green bar: leaf period; vertical yellow-line bar: flowering; diagonal brown-line bar: fruiting; and brown bar: leaf senescence. e) Daily precipitation in the study area. f) Monthly mean normalized difference vegetation index (NDVI) of the canopy (dark circles) and inter-canopy (light ones).

Table 2
Mean soil carbon biomass and soil mineralization rate, after 23 days of incubation (± SE), differentiating between under- and inter-canopy. *F*-statistic and significance of the ANOVA are shown (***$P < 0.001$).

	Under-canopy	Inter-canopy	*F*	Significance
C_{mic} (mg kg^{-1} soil)	7.51 ± 0.13	3.90 ± 0.02	729.6	***
Mineralization rate[a] ($\mu gCO_2\ g^{-1}$ soil h^{-1})	114.81 ± 7.79	7.15 ± 1.03	459.6	***

[a] After incubating for 23 days.

were also found here as total nitrogen (N_{tot}), whereas the ratio C:N was not significantly different between sites ($P = 0.07$).

Between the soil solution components, the difference between canopy conditions was variable. Regarding nitrates (NO_3^-), under-canopy soils showed higher concentrations, whereas neither nitrites (NO_2^-) nor sulfate (SO_4^{2-}) concentrations showed spatial differences. In the case of phosphate (PO_4^{3-}), we did not observe signals of this element inter-canopy whereas the mean value obtained under-canopy came from 2 of the 4 monitored patches.

We found positive regressions between soil carbon and mineralization rates (Fig. 4). Generally, higher concentrations of WEOC and TOC were related to higher initial pulse of CO_2 (mineralization rate in 1 h) ($R^2 = 0.71$, $P < 0.001$, $df = 22$; $R^2 = 0.65$, $P < 0.001$, $df = 22$, respectively) (Fig. 4a, b). However, these relationships varied between covers, since the initial pulse of CO_2 was only related to WEOC under-canopy ($R^2 = 0.64$, $P = 0.002$, $df = 1,10$; Fig. 4a), and to TOC inter-canopy ($R^2 = 0.65$, $P = 0.001$, $df = 1,10$; Fig. 4b). Similarly, the total mineralization rate after 23 days was significantly related with WEOC ($R^2 = 0.56$, $P < 0.001$, $df = 22$) and TOC ($R^2 = 0.65$, $P < 0.001$, $df = 22$) (Fig. 4c, d), although in this case the particular significant regression occurred just with TOC inter-canopy ($R^2 = 0.63$, $P = 0.002$, $df = 1,10$) (Fig. 4d).

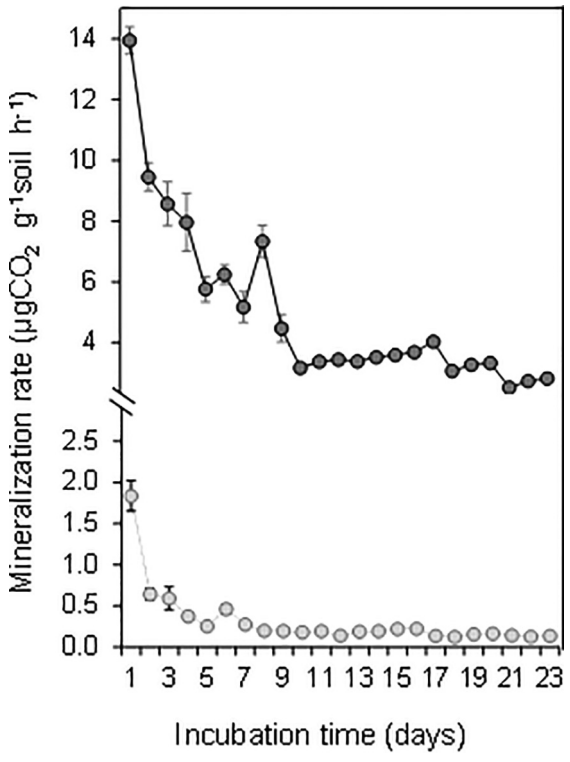

Fig. 3. Dynamic of soil mineralization rate ($\mu gCO_2\ g^{-1}$ soil h^{-1}) during 23-day incubation experiment. Mean values (±SE) under-canopy (dark circles) and inter-canopy (light ones) are shown.

Table 3
Mean values of the soil organics fractions (total organic carbon, TOC; water extractable organic carbon, WEOC; total nitrogen, Ntot; ratio carbon:nitrogen, C:N) and main components in soil solution (nitrate, NO_3^-; nitrite, NO_2^-; sulphate, SO_4^{2-}; phosphate, PO_4^{3-}) (±SE), differentiating between under- and inter-canopy. F-statistic and significance of the ANOVA are shown (***$P < 0.001$, ns: non-significant, na: non-assessed).

	Under-canopy	Inter-canopy	*F*	Significance
Soil organic fraction				
TOC (g kg^{-1} soil)	8.00 ± 0.88	1.27 ± 0.15	57.26	***
WEOC (g kg^{-1} soil)	0.14 ± 0.01	0.05 ± 0.01	32.27	***
N_{tot} (g kg^{-1} soil)	0.73 ± 0.09	0.13 ± 0.01	35.79	***
C:N	11.37 ± 0.65	9.45 ± 0.74	3.76	ns
Soil solution components				
NO_3^- (mg kg^{-1} soil)	9.20 ± 1.24	0.62 ± 0.04	81.11	***
NO_2^- (mg kg^{-1} soil)	0.21 ± 0.03	0.57 ± 0.32	3.34	ns
SO_4^{2-} (mg kg^{-1} soil)	112.9 ± 18.9	95.4 ± 12.8	0.51	ns
PO_4^{3-} (mg kg^{-1} soil)	3.04 ± 0.22	–	–	na

4. Discussion

4.1. Soil and vegetation dynamics in a groundwater-dependent ecosystem in drylands

Our study showed how soil and vegetation dynamics in a GDE in drylands mostly respond to water availability. Whereas soil biological activity highly depends on precipitation and promptly responded to significant events, vegetation activity relies on less superficial water and responded on different time scales.

Differences in soil respiration (Rs) throughout the year can largely be explained by variations in soil water content (SWC), whose temporal variability was coupled to precipitation pulses (Vargas et al., 2018). Rainfall, and thus soil moisture, is one of the main drivers of Rs in most arid and semiarid ecosystems (Austin et al., 2004; Morillas et al., 2017; Noy-Meir, 1973; Rey et al., 2011; Rey et al., 2021), as is it in this arid GDE due to the effect of rewetting associated with precipitation events (Birch effect; Birch, 1959). Soil moisture increases can rapidly stimulate Rs, and particularly its heterotrophic component, by increasing decomposition processes of readily available carbon products that accumulate in the soil during previous dry periods (Austin et al., 2004; Sponseller, 2007). We detected two major soil CO_2 effluxes in autumn and spring when some precipitation events increased SWC. This effect has already been recorded in this semiarid region for grasslands and shrubs (Rey et al., 2011; Rey et al., 2021). In October, we might expect that the accumulation of labile carbon and microbial biomass during summer, due to reduced soil moisture and the interruption of biological decomposition, would foster greater Rs when SWC increases (Austin et al., 2004). However, the precipitation event that occurred at the beginning of September (16.3 mm), which could have driven the consumption of such accumulated carbon, fostered a lower response if compared with the one in April. The timing between the rainfall of September and the measurement can explain such difference (Table S2). The effect of rewetting could have been underrepresented because soil CO_2 effluxes in arid and semiarid ecosystems can swiftly return to pre-rain values within a few days (Sponseller, 2007). In April, after a long period with low SWC, a high precipitation pulse was recorded (10.4 mm) and the timing between it and the measurement was shorter (Table S2), which could have promoted the record of such an intense response. Therefore, the magnitude of the precipitation events, and mostly the interval between them determine CO_2 efflux in drylands (Sponseller, 2007), which showed a lack of seasonality derived from the precipitation pulses (Vargas et al., 2018).

Soil temperature also affected Rs, although to a lesser extent, as described by other studies in the area (Oyonarte et al., 2012; Rey et al., 2011). Soil temperature can directly increase Rs, although several studies have reported that temperature sensitivity of Rs can decrease when some thresholds are surpassed (15 °C, Conant et al., 2004; 20 °C, Rey et al., 2011, Oyonarte et al., 2012). Additionally, temperature might be only

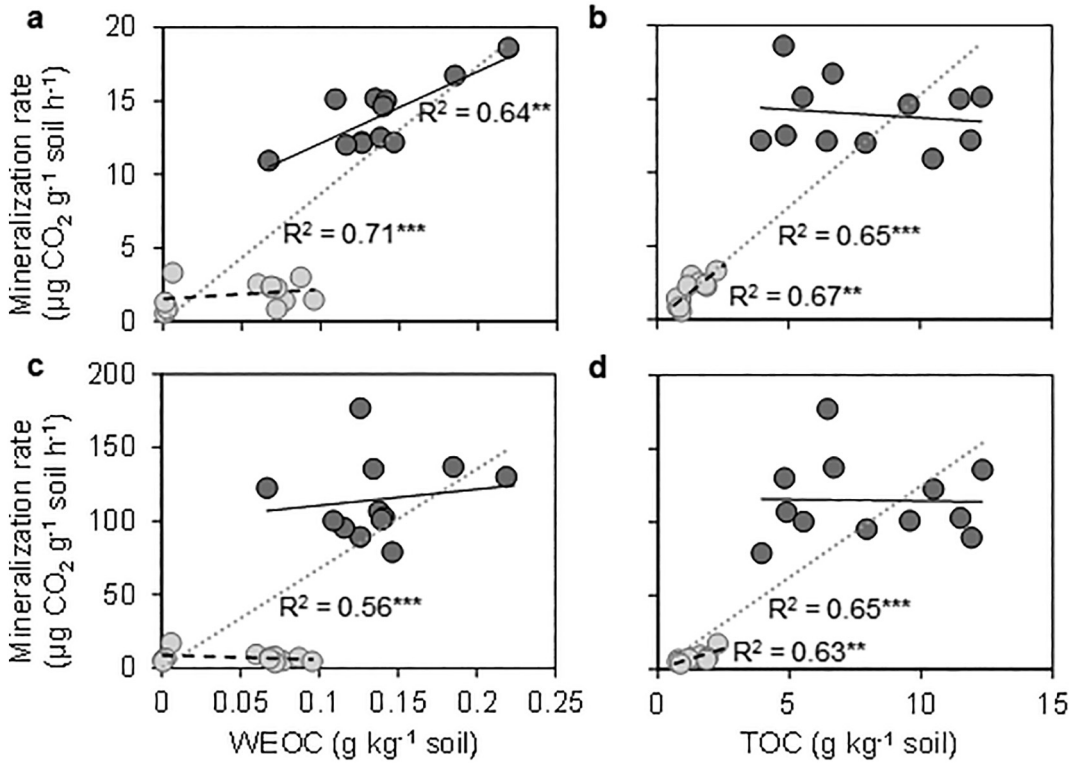

Fig. 4. Relationships between soil organics fractions and soil mineralization rates at the beginning of the experiment (1 h) (a–b) and after 23 days (c–d). Panels a and c refer to water extractable organic carbon (WEOC) and b and d to total organic carbon (TOC). Dark circles represent under-canopy values and light ones, inter-canopy. Grey dotted lines show general regressions, whereas solid black line refers to under-canopy regressions and dashed black lines to inter-canopy ones. The goodness of the fit (R^2) and *P*-value are shown next to its regression line when significant. Significance: $^{***}P < 0.001$, $^{**}P < 0.01$.

relevant when there is sufficient soil moisture for microbial activity (Almagro et al., 2009). Thus, it is likely that in our study, the high soil temperature (above 20 °C during most of the year) and the generally low SWC would have reduced the effect of temperature on Rs.

Litter and organic matter can also determine microbial decomposition rates and Rs (Gallardo and Schlesinger, 1992). The decrease in vegetation activity, represented by lower NDVI values, might indicate litter inputs from both winter and summer deciduous species of the GDE (minimum NDVI in September and March respectively). Associated to that inputs, and to precipitation events, CO_2 effluxes occurred (October and April). Vegetation from arid and semiarid regions around the world usually show a seasonal unimodal pattern with maximum values of primary productivity that coincide with rainy periods (either spring, see Lopez-Ballesteros et al., 2017; or winter, Holm et al., 2003; Gaitan et al., 2021). However, the groundwater connection of phreatophytes fosters another maximum (early summer in this GDE) and a bimodal pattern of the vegetation activity. Moreover, phreatophytes produce higher biomass than expected for an arid ecosystem (Barron et al., 2014). Therefore, the capacity to incorporate litter and organic matter into the soil in arid regions is enhance in GDEs. Whereas SWC is needed for stimulating soil biological activity, groundwater is essential to provide the substrate for such activity and thus, to promote biogeochemical cycles in drylands.

4.2. Fertile island effect on soil biological activity and soil quality

Soil CO_2 effluxes and environmental conditions differed spatially because of vegetation and soil heterogeneity that characterize these dryland ecosystems (Austin et al., 2004). As expected, higher CO_2 effluxes were observed under-canopy, and the differences with inter-canopy rates increased during wet periods (October and April). Such spatial differences can be explained by higher root density, but also organic carbon and nutrients that largely accumulate under-canopy as a result of litter deposition, soil biota mineralization, and decomposition (Sponseller, 2007; Tucker and Reed, 2016). However, these effects are difficult to separate in the field, and particularly when SWC is limiting.

Inter-canopy soils showed higher SWC than under-canopy ones. Phreatophytes in arid and semiarid environments can contribute to enhancing SWC under-canopy because large canopies shade direct sun radiation, prevent high soil temperatures, and increase soil moisture content (Cao et al., 2016). Nonetheless, the great vegetation density in the patches, and the high transpiration rate of species such as *Z. lotus* (Torres-García et al., 2021b) will deplete soil water faster under-canopy (Martínez-Vilalta and Garcia-Forner, 2017). Contrary, bare soils, which are highly exposed to the evaporative component, can maintain wetter conditions on the near surface since the loss of water by capillarity can be interrupted because of the absence of the transpirative component. In any case, CO_2 effluxes were higher under-canopy, since the amount of available material to be decomposed, which barely accumulates inter-canopy, limits soil biological activity and carbon pulses (Gallardo and Schlesinger, 1992; Rey et al., 2017).

When removing the autotrophic component and water limitation by bringing the soils into the laboratory, the carbon fluxes might be attributed to the carbon substrate, microbial biomass, and mineralization rates (Butterly et al., 2009; Gallardo and Schlesinger, 1992). The higher organic carbon (both TOC and WEOC) under-canopy is related to vegetation cover and its litter inputs, whereas the low and scarcely mineralizable organic carbon observed inter-canopy supports the hypothesis that nutrients and organic matter availability is limited outside the canopy. Additionally, both carbon fractions were positively related to mineralization rates, since TOC and WEOC inform about the degree of organic matter decomposition (Embacher et al., 2007). Thus, the labile carbon fraction was related to the first stage of mineralization rate (the first hour of incubation) under-canopy because of higher microbial biomass that easily decomposes such fraction. Contrary, TOC was related to the mineralization rate inter-canopy, both at the beginning of the mineralization and after the 23-day accumulation process. Therefore, not only the amount of soil carbon

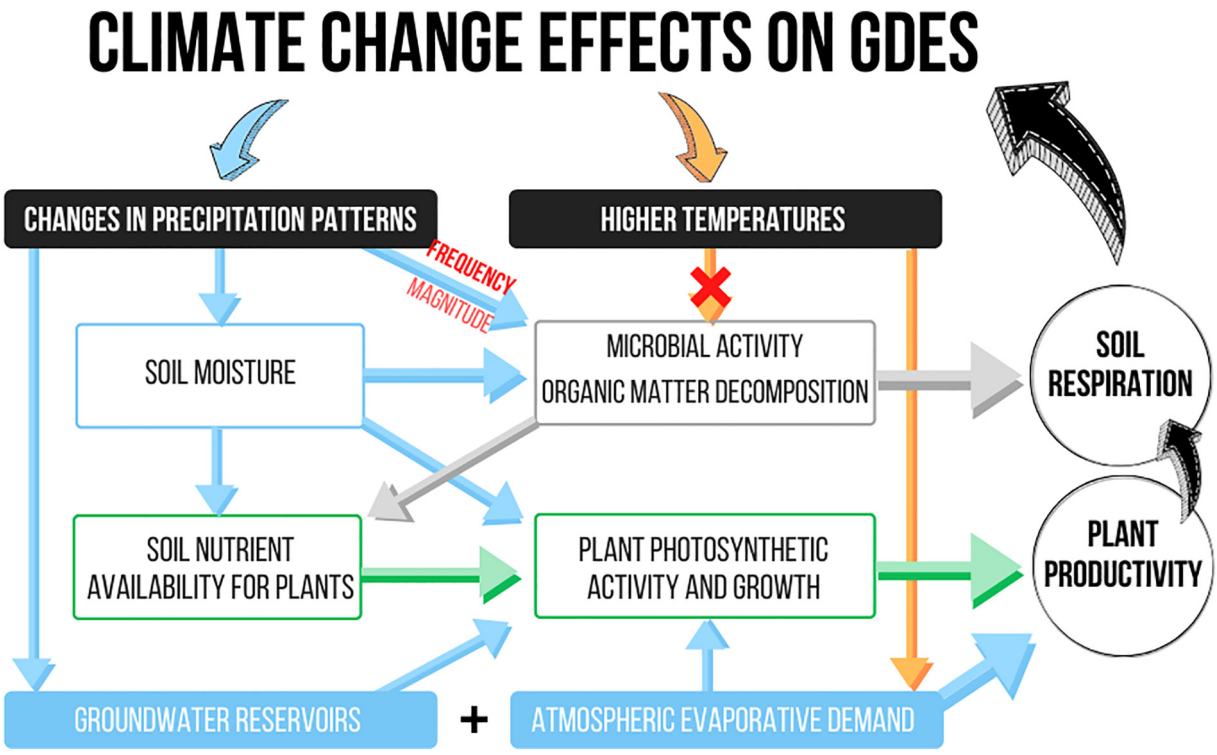

Fig. 5. Conceptual diagram of climate change effects over groundwater-dependent ecosystems (GDEs) from the literature (Bardgett et al., 2013; Querejeta et al., 2021) and the results obtained from this study (red marks). Bluish sections refer to water components, whereas greenish and greyish ones represent plant and soil components respectively.

determines the carbon fluxes, but also the way that carbon is available for microbial decomposition (Rey et al., 2017).

The larger amount of litter that accumulates under-canopy promotes a spatial heterogeneity in the microbial biomass and their decomposition rates (Gallardo and Schlesinger, 1992). The fast mineralization rates observed under-canopy when soil moisture is maintained (from 13.95 to 3.17 $\mu gCO_2\ g^{-1}$ soil h^{-1} in 9 days) evidence a pattern similar to those occurring in tropical forests when organic carbon is swiftly decomposed (e.g., Whitaker et al., 2014). Moreover, the reduction in the mineralization rates and the oscillating pattern observed might reflect shifts in the microbial community composition (Butterly et al., 2009) combined with the consumption of labile carbon first, and more recalcitrant sources later. In fact, soil microbial communities are commonly more functionally diverse under-canopy than in bare soils (Garcia et al., 2018). Overall, both the quantity and quality of litter inputs determine the diversity in soil microbial communities (Ochoa-Hueso et al., 2018) and the rates of carbon and nitrogen cycling (Chen and Stark, 2000). Soil microbial diversity and the nutrient cycling might be enhanced here by combining the morpho-functional distinct leaves of *Z. lotus* (leaves with high and low specific leaf areas and decomposition rates, Pérez-Harguindeguy et al., 2013) and the litter of associated summer-deciduous species (Torres-García et al., 2021c). The mineralization of carbon and nitrogen is a fundamental biogeochemical process that maintains the fertility of the soil under the plants, and which products are essential for increasing vegetation biomass production and decreasing the risk, extent, and severity of desertification (Lal, 2003).

Soil quality (i.e., physical-chemical properties strongly related to soil organic carbon pool and desertification process, Lal, 2001) can also determine differences in CO_2 effluxes (Oyonarte et al., 2012). Coarser soil texture, lower organic carbon content, and hence lower biological activity can contribute to CO_2 diffusion within the soil and to increase carbon fluxes to the atmosphere during dry periods (Oyonarte et al., 2012). Overall, desert soils in arid and semiarid regions typically have low organic carbon and total nitrogen concentrations as a consequence of low contents of silt and clay (Wang et al., 2019). Additionally, the reduced vegetation cover and productivity derived from aridity, promote the heterogeneity of carbon inputs to the soil (Ruiz Sinoga et al., 2012). The higher content of sand found inter-canopy and the higher erosion susceptibility of these areas might have reduced the retention capacity of nutrients (Lal, 2001; Campos et al., 2020). Contrary, the formation of *nebkhas* (i.e. coppice dunes) promote the accumulation of sediments, organic carbon, and nutrients under-canopy (Wang et al., 2019), as reflected in our results (higher WEOC, TOC, NO_3^-, and N_{tot}). Indeed, the concentration of NO_3^- and PO_4^{3-} under-canopy were much larger than the mean values of other Mediterranean shrublands (Morillas et al., 2017). Since phreatophytes have more reliable access to water than non-phreatophyte species of arid regions, primary productivity and vegetation biomass are enhanced, as are nutrient availability and soil fertility in vegetation patches. Therefore, our outcomes are consistent with the well-known 'fertile islands' definition (Maestre et al., 2001; Ochoa-Hueso et al., 2018), and with the possibility that *Z. lotus* enhances soil quality in drylands.

4.3. Implications for conservation under climate change

Terrestrial ecosystems of arid and semiarid regions are highly vulnerable to soil degradation and desertification (Rey et al., 2011; Martínez-Valderrama et al., 2020), in spite of the beneficial effect of fertile islands (Lal, 2001). Global warming will alter global air circulation patterns, which will affect precipitation regimes across scales, reducing rainfall amounts in the Mediterranean basin and prolonging drought periods (Guiot and Cramer, 2016). Such effects will limit soil moisture and groundwater recharge (Eamus et al., 2006), which can cause groundwater declines if transpiration rates of phreatophytic vegetation are maintained (Nichols, 1994). When soil moisture and/or groundwater sources are reduced, vegetation growth in GDEs is limited, hence the supply of organic matter into the soil, which drives lower nutrients, structural stability, and water holding capacity (Ruiz Sinoga et al., 2012). In drylands, precipitation frequency will particularly alter soil respiration (Vargas et al., 2018) as well as soil

microbial activity and organic matter decomposition (Prieto et al., 2019), also in GDEs (Fig. 5).

Higher temperatures would increase atmospheric evaporative demand, and hence, plant photosynthetic activity and growth when water availability is guaranteed (Torres-García et al., 2021a; Wu et al., 2011). In the case of the phreatophyte *Z. lotus*, higher atmospheric evaporative demand would increase photosynthetic and transpiration rates, but also groundwater uptake when it is easily available (groundwater depth < 13 m in the study area) (Torres-García et al., 2021a, 2021b). Atmospheric CO_2 increases can also stimulate plant growth, root respiration, and organic matter mineralization, contributing to soil carbon losses (Bardgett et al., 2013). However, reduced precipitation, soil moisture, and groundwater availability (groundwater discharge due to phreatophytic transpiration and groundwater exploitation), might compromise both soil-nutrient availability and plant productivity (Querejeta et al., 2021).

Prolonged droughts during summer can diminish nutrient uptake for species with dimorphic root systems (Querejeta et al., 2021) such as *Z. lotus,* since plant nutrient uptake and accumulation in leaves depend on water availability (Salazar-Tortosa et al., 2018). Because of its winter-deciduousness, *Z. lotus* has limited wet periods when obtaining water and nutrients from the topsoil (Torres-García et al., 2021b). Reduced nutrient acquisition can drive lower accumulation of nutrients on leaves, which could also contribute to reducing litter quality. Changes in plant traits can alter the functional composition of the associated soil microbial community, thus driving changes in decomposition and mineralization processes (de Bello et al., 2010). In a final stage, severe groundwater declines can cause extensive mortality if roots are separated from the water source (Naumburg et al., 2005). The loss of *Z. lotus* plants might promote low-quality, heterogeneous soils like inter-canopy ones, which would increase the effect of desertification. This cascade of disturbances might severely affect soil respiration patterns in drylands, particularly in those ecosystems that rely on groundwater, altering carbon cycles globally (Bardgett et al., 2013), hence fostering climate change effects.

5. Conclusions

In this study we show how soil and vegetation dynamics in a groundwater-dependent ecosystem (GDE) in semiarid regions mostly respond to water availability. Whereas soil biological activity highly depends on soil moisture and promptly responded to precipitation events, vegetation activity relies on less superficial water and responded on different time scales. The greater effect of soil moisture on soil biological activity suggests the importance of water resources to foster the functioning of the soil component. However, groundwater connection is essential to provide the substrate for such activity (i.e., litter inputs) and thus, to enhance biogeochemical cycles in drylands. Soil activity as well as carbon fractions and nutrients were higher in the patches of vegetation (under-canopy) than in bare soils (inter-canopy), highlighting the 'fertile island' effect promoted by the phreatophytic vegetation. Overall, phreatophytic vegetation in the GDEs enhances soil quality and microbial composition in drylands under a continuous organic matter input (under-canopy). Thus, the influence of groundwater connection does not go beyond the vegetation patch. However, our findings expose the vulnerability of arid GDEs to climate change effects and land degradation, due to the dependence of soil biological processes on precipitation for activation, and on phreatophytic vegetation and its groundwater connection for litter input and soil quality. The loss of one fertile island in drylands could be detrimental to the functional diversity of these ecosystems, since it might drive irreversible changes in processes such as soil microbial activity, organic matter mineralization, and productivity.

Credit authorship contribution statement

MTT, CO, JC and MJS conceived the study. MTT and MJS conducted fieldwork. MTT conducted laboratory experiments with BR. EG developed remote sensing analysis. MTT analysed data and wrote the manuscript with input and revision of all authors.

Declaration of competing interest

The authors declare that they have no known competing financial interests or personal relationships that could have appeared to influence the work reported in this paper.

Acknowledgments

The authors thank Francisco Martín Belmonte from the University of Almería who helped with soil sample preparation and Manuel Salvador who assisted with laboratory analysis. We also thank the anonymous reviewers that substantially contribute to enhance this manuscript during the publication procedure.

Funding

This research was developed in the framework of the LTSER Platform "The Arid Iberian South East LTSER Platform — Spain (LTER_ EU_ES_027)" and supported by the European project LIFE Adaptamed (LIFE14349610 CCA/ES/000612). MTT and BRL were financially supported by a FPU Predoctoral Fellowship of the Spanish Government (16/02214 and 17/01886). EG was supported by the European Research Council (ERC Grant agreement 647038 [BIODESERT]).

Appendix A. Supplementary data

Supplementary data to this article can be found online at https://doi.org/10.1016/j.scitotenv.2022.154111.

References

Aguiar, M.R., Sala, O.E., 1999. Patch structure, dynamics and implications for the functioning of arid ecosystems. Trends Ecol. Evol. 14 (7), 273–277. https://doi.org/10.1016/S0169-5347(99)01612-2.

Almagro, M., Lopez, J., Querejeta, J.I., Martinez-Mena, M., 2009. Temperature dependence of soil CO2 efflux is strongly modulated by seasonal patterns of moisture availability in a Mediterranean ecosystem. Soil Biol. Biochem. 41, 594–605. https://doi.org/10.1016/j.soilbio.2008.12.021.

Anderson, J.P.E., Domsch, K.H., 1978. A physiological method for the quantitative measurement of microbial biomass in soils. Soil Biol. Biochem. 10, 215–221. https://doi.org/10.1016/0038-0717(78)90099-8.

Antunes, C., Chozas, S., West, J., Zunzunegui, M., Diaz Barradas, M.C., Vieira, S., Máguas, C., 2018. Groundwater drawdown drives ecophysiological adjustments of woody vegetation in a semi-arid coastal ecosystem. Glob. Chang.Biol. 24, 4894–4908. https://doi.org/10.1111/gcb.14403.

Austin, A.T., Yahdjian, L., Stark, J.M., Belnap, J., Porporato, A., Norton, U., Ravetta, D.A., Schaeffer, S.M., 2004. Water pulses and biogeochemical cycles in arid and semiarid ecosystems. Oecologia 141, 221–235. https://doi.org/10.1007/s00442-004-1519-1.

De Baets, S., Poesen, J., Knapen, A., Barberá, G.G., Navarro, J.A., 2007. Root characteristics of representative Mediterranean plant species and their erosion-reducing potential during concentrated runoff. Plant Soil 294, 169–183. https://doi.org/10.1007/s11104-007-9244-2.

Bardgett, R.D., Manning, P., Morriën, E., De Vries, F.T., 2013. Hierarchical responses of plant-soil interactions to climate change: consequences for the global carbon cycle. J. Ecol. 101, 334–343. https://doi.org/10.1111/1365-2745.12043.

Barron, O.V., Emelyanova, I., Van Niel, T.G., Pollock, D., Hodgson, G., 2014. Mapping groundwater-dependent ecosystems using remote sensing measures of vegetation and moisture dynamics: GDEs mapping using remote measures of vegetation/moisture dynamics. Hydrol. Process. 28, 372–385. https://doi.org/10.1002/hyp.9609.

de Bello, F., Lavorel, S., Díaz, S., Harrington, R., Cornelissen, J.H.C., Bardgett, R.D., Berg, M.P., Cipriotti, P., Feld, C.K., Hering, D., Martins da Silva, P., Potts, S.G., Sandin, L., Sousa, J.P., Storkey, J., Wardle, D.A., Harrison, P.A., 2010. Towards an assessment of multiple ecosystem processes and services via functional traits. Biodivers. Conserv. 19, 2873–2893. https://doi.org/10.1007/s10531-010-9850-9.

Birch, H., 1959. The effect of soil drying on humus decomposition and nitrogen availability. Plant Soil 12, 9–31. https://doi.org/10.1007/BF01343734.

Butterly, C.R., Bünemann, E.K., McNeill, A.M., Baldock, J.A., Marschner, P., 2009. Carbon pulses but not phosphorus pulses are related to decreases in microbial biomass during repeated drying and rewetting of soils. Soil Biol. Biochem. 41, 1406–1416. https://doi.org/10.1016/j.soilbio.2009.03.018.

Campos, C.A., Suárez, M.G., Laborde, J., 2020. Analyzing vegetation cover-induced organic matter mineralization dynamics in sandy soils from tropical dry coastal ecosystems. Catena 185, 104264. https://doi.org/10.1016/j.catena.2019.104264.

Cao, C., Abulajiang, Y., Zhang, Y., Feng, S., Wang, T., Ren, Q., Li, H., 2016. Assessment of the effects of phytogenic nebkhas on soil nutrient accumulation and soil microbiological

property improvement in semi-arid sandy land. Ecol. Eng. 91, 582–589. https://doi.org/10.1016/j.ecoleng.2016.03.042.
Chen, J., Stark, J.M., 2000. Plant species effects and carbon and nitrogen cycling in a sagebrush-crested wheatgrass soil. Soil Biol. Biochem. 32, 47–57. https://doi.org/10.1016/S0038-0717(99)00124-8.
Colvin, C., Le Maitre, D., Hughes, S., 2003. Assessing Terrestrial Groundwater Dependent Ecosystems in South Africa. Water Research Commission WRC Report No. 1090-2/03.
Conant, R.T., Dalla-Bettab, P., Klopatekc, C.C., Klopatekd, J.M., 2004. Controls on soil respiration in semiarid soils. Soil Biol. Biochem. 35, 945–951. https://doi.org/10.1016/j.soilbio.2004.02.013.
Delgado-Baquerizo, M., Maestre, F.T., Gallardo, A., Bowker, M.A., Wallenstein, M.D., Quero, J.L., Ochoa, V., Gozalo, B., García-Gómez, M., Soliveres, S., García-Palacios, P., Berdugo, M., Valencia, E., Escolar, C., Arredondo, T., Barraza-Zepeda, C., Bran, D., Carreira, J.A., Chaieb, M., Conceição, A.A., Derak, M., Eldridge, D.J., Escudero, A., Espinosa, C.I., Gaitán, J., Gatica, M.G., Gómez-González, S., Guzman, E., Gutiérrez, J.R., Florentino, A., Hepper, E., Hernández, R.M., Huber-Sannwald, E., Jankju, M., Liu, J., Mau, R.L., Miriti, M., Monerris, J., Naseri, K., Noumi, Z., Polo, V., Prina, A., Pucheta, E., Ramírez, E., Ramírez-Collantes, D.A., Romão, R., Tighe, M., Torres, D., Torres-Díaz, C., Ungar, E.D., Val, J., Wamiti, W., Wang, D., Zaady, E., 2013. Decoupling of soil nutrient cycles as a function of aridity in global drylands. Nature 502, 672–676. https://doi.org/10.1038/nature12670.
Delgado-Baquerizo, M., Maestre, F.T., Reich, P.B., Jeffries, T.C., Gaitan, J.J., Encinar, D., Berdugo, M., Campbell, C.D., Singh, B.K., 2016. Microbial diversity drives multifunctionality in terrestrial ecosystems. Nat. Commun. 7, 10541. https://doi.org/10.1038/ncomms10541.
Eamus, D., Froend, R., Loomes, R., Hose, G., Murray, B., 2006. A functional methodology for determining the groundwater regime needed to maintain the health of groundwater-dependent vegetation. Aust. J. Bot. 54, 97. https://doi.org/10.1071/BT05031.
Embacher, A., Zsolnay, A., Gattinger, A., Munch, J.C., 2007. The dynamics of water extractable organic matter (WEOM) in common arable topsoils: I. Quantity, quality and function over a three year period. Geoderma 139, 11–22. https://doi.org/10.1016/j.geoderma.2006.12.002.
Gaitan, J., Ciano, N., Oliva, G., Bran, D., Butti, L., Cariac, G., Caruso, C., Opazo, W., Ferrante, D., Echevarria, D., Buono, G., Fantozzi, A., Guirado, E., Maestre, F., 2021. La variación temporal del índice NDVI predice los cambios temporales de la cobertura vegetal en las tierras secas de la Patagonia Argentina. Ecosistemas 30 (3), 2229. https://doi.org/10.7818/ECOS.2229.
Gallardo, A., Schlesinger, W.H., 1992. Carbon and nitrogen limitations of soil microbial biomass in desert ecosystems. Biogeochemistry 18, 1–17. https://doi.org/10.1007/BF00000423.
Garcia, D.E., Lopez, B.R., de-Bashan, L.E., Hirsch, A.M., Maymon, M., Bashan, Y., 2018. Functional metabolic diversity of the bacterial community in undisturbed resource island soils in the southern Sonoran Desert. Land. Degrad. Dev. 29, 1467–1477. https://doi.org/10.1002/ldr.2905.
Glenn, E.P., Nagler, P.L., Morino, K., Hultine, K.R., 2013. Phreatophytes under stress: transpiration and stomatal conductance of saltcedar (Tamarix spp.) in a high-salinity environment. Plant Soil 371, 655–673.
Guirado, E., Alcaraz-Segura, D., Rigol-Sánchez, J.P., Gisbert, J., Martínez-Moreno, F.J., Galindo-Zaldívar, J., González-Castillo, L., Cabello, J., 2018. Remote-sensing-derived fractures and shrub patterns to identify groundwater dependence. Ecohydrology 11, e1933. https://doi.org/10.1002/eco.1933.
Guirado, E., Blanco-Sacristán, J., Rigol-Sánchez, J.P., Alcaraz-Segura, D., Cabello, J., 2019. A multi-temporal object-based image analysis to detect long-lived shrub cover changes in drylands. Remote Sens. 11 (22), 2649. https://doi.org/10.3390/rs11222649.
Guirado, E., Tabik, S., Alcaraz-Segura, D., Cabello, J., Herrera, F., 2017. Deep-learning versus OBIA for scattered shrub detection with Google Earth Imagery: Ziziphus lotus as case study. Remote Sens. 9 (12), 1220. https://doi.org/10.3390/rs9121220.
Guiot, J., Cramer, W., 2016. Climate change: the 2015 Paris Agreement thresholds and Mediterranean basin ecosystems. Science 354, 4528–4532. https://doi.org/10.1126/science.aah5015.
Holm, A.M., Cridland, S.W., Roderick, M.L., 2003. The use of time-integrated NOAA NDVI data and rainfall to assess landscape degradation in the arid shrubland of Western Australia. Remote Sens. Environ. 85, 145–158. https://doi.org/10.1016/S0034-4257(02)00199-2.
Lal, R., 2001. Potential of desertification control to sequester carbon and mitigate the greenhouse effect. In: Rosenberg, N.J., Izaurralde, R.C. (Eds.), Storing Carbon in Agricultural Soils: A Multi-purpose Environmental Strategy. Springer, Netherlands, Dordrecht, pp. 35–72 https://doi.org/10.1007/978-94-017-3089-1_3.
Lal, R., 2003. Global potential of soil carbon sequestration to mitigate the greenhouse effect. Crit. Rev. Plant Sci. 22, 151–184. https://doi.org/10.1080/713610854.
Lambers, H., Oliveira, R.S., 2019. Plant Physiological Ecology. Springer International Publishing, Cham https://doi.org/10.1007/978-3-030-29639-1.
Lang, L., Wang, X., Hasi, E., Hua, T., 2013. Nebkha (coppice dune) formation and significance to environmental change reconstructions in arid and semiarid areas. J. Geogr. Sci. 23, 344–358. https://doi.org/10.1007/s11442-013-1014-x.
Le Houérou, H.N., 2006. Agroforestry and silvopastoralism: the role of trees and shrubs (Trubs) in range rehabilitation and development. Sci.ChangPlanét. 17, 343–348.
Lopez-Ballesteros, A., Serrano-Ortiz, P., Kowalski, A.S., Oyonarte, C., Sanchez-Cañete, E.P., Moya, M.R., Domingo, F., 2017. How land degradation affects the carbon balance and its component processes: a case of study in SE Spain. Biogeosciences https://doi.org/10.5194/bg-2017-77.
Machado, M.J., Benito, G., Barriendos, M., Rodrigo, F.S., 2011. 500 years of rainfall variability and extreme hydrological events in southeastern Spain drylands. J. Arid Environ. 75, 1244–1253. https://doi.org/10.1016/j.jaridenv.2011.02.002.
Maestre, F.T., Bautista, S., Cortina, J., Bellot, J., 2001. Potential for using facilitation by grasses to establish shrubs on a semiarid degraded steppe. Ecol. Appl. 11, 1641–1655. https://doi.org/10.1890/1051-0761(2001)011[1641:PFUFBG]2.0.CO;2.
Martín, J., Escarré, A., 1980. Datos de fenología, reducción de hoja y variaciones estacionales de la composición foliar, en cuatro especies del matorral costero del Mediterráneo meridional ibérico. Mediterránea. Serie de Estudios sobre Biología Terrestre Mediterránea4, pp. 69–87 ISSN 0210-5004.
Martínez-Valderrama, J., Guirado, E., Maestre, F.T., 2020. Desertifying deserts. Nat. Sustain. 3, 572–575. https://doi.org/10.1038/s41893-020-0561-2.
Martínez-Vilalta, J., Garcia-Forner, N., 2017. Water potential regulation, stomatal behaviour and hydraulic transport under drought: deconstructing the iso/anisohydric concept: deconstructing the iso/anisohydric concept. Plant Cell Environ. 40, 962–976. https://doi.org/10.1111/pce.12846.
Mingorance, M.D., Barahona, E., Fernández-Gálvez, J., 2007. Guidelines for improving organic carbon recovery by the wet oxidation method. Chemosphere 68 (3), 409–413. https://doi.org/10.1016/j.chemosphere.2007.01.021.
Morillas, L., Roales, J., Portillo-Estrada, M., Gallardo, A., 2017. Wetting-drying cycles influence on soil respiration in two Mediterranean ecosystems. Eur. J. Soil Biol. 82, 10–16. https://doi.org/10.1016/j.ejsobi.2017.07.002.
Naumburg, E., Mata-gonzalez, R., Hunter, R.G., McLendon, T., Martin, D.W., 2005. Phreatophytic vegetation and groundwater fluctuations: a review of current research and application of ecosystem response modeling with an emphasis on Great Basin vegetation. Environ. Manag. 35, 726–740. https://doi.org/10.1007/s00267-004-0194-7.
Newman, B.D., Wilcox, B.P., Archer, S.R., Breshears, D.D., Dahm, C.N., Duffy, C.J., McDowell, N.G., Phillips, F.M., Scanlon, B.R., Vivoni, E.R., 2006. Ecohydrology of water-limited environments: a scientific vision. Water Resour. Res. 42, W06302. https://doi.org/10.1029/2005WR004141.
Nichols, W.D., 1994. Groundwater discharge by phreatophyte shrubs in the Great Basin as related to depth to groundwater. Water Resour. Res. 30, 3265–3274. https://doi.org/10.1029/94wr02274.
Noy-Meir, I., 1973. Desert ecosystems: environment and producers. Ann. Rev. Ecol. Syst. 4, 25–51. https://doi.org/10.1146/annurev.es.04.110173.000325.
Ochoa-Hueso, R., Eldridge, D.J., Delgado-Baquerizo, M., Soliveres, S., Bowker, M.A., Gross, N., Le Bagousse-Pinguet, Y., Quero, J.L., García-Gómez, M., Valencia, E., Arredondo, T., Beinticinco, L., Bran, D., Cea, A., Coaguila, D., Dougill, A.J., Espinosa, C.I., Gaitán, J., Guuroh, R.T., Guzman, E., Gutiérrez, J.R., Hernández, R.M., Huber-Sannwald, E., Jeffries, T., Linstädter, A., Mau, R.L., Monerris, J., Prina, A., Pucheta, E., Stavi, I., Thomas, A.D., Zaady, E., Singh, B.K., Maestre, F.T., 2018. Soil fungal abundance and plant functional traits drive fertile island formation in global drylands. J. Ecol. 106, 242–253. https://doi.org/10.1111/1365-2745.12871.
Orellana, F., Verma, P., Loheide, S.P., Daly, E., 2012. Monitoring and modeling water-vegetation interactions in groundwater-dependent ecosystems: groundwater-dependent ecosystems. Rev. Geophys. 50, RG3003. https://doi.org/10.1029/2011RG000383.
Oyonarte, C., Rey, A., Raimundo, J., Miralles, I., Escribano, P., 2012. The use of soil respiration as an ecological indicator in arid ecosystems of the SE of Spain: spatial variability and controlling factors. Ecol. Indic. 14, 40–49. https://doi.org/10.1016/j.ecolind.2011.08.013.
Paruelo, J.M., Epstein, H.E., Lauenroth, W.K., Burke, I.C., 1997. ANPP estimates from NDVI for the central grassland region of the United States. Ecology 78, 953–958. https://doi.org/10.2307/2266073.
Pérez-Harguindeguy, N., Díaz, S., Garnier, E., Lavorel, S., Poorter, H., Jaureguiberry, P., Bret-Harte, M.S., Cornwell, W.K., Craine, J.M., Gurvich, D.E., Urcelay, C., Veneklaas, E.J., Reich, P.B., Poorter, L., Wright, I.J., Ray, P., Enrico, L., Pausas, J.G., de Vos, A.C., Buchmann, N., Funes, G., Quétier, F., Hodgson, J.G., Thompson, K., Morgan, H.D., ter Steege, H., Sack, L., Blonder, B., Poschlod, P., Vaieretti, M.V., Conti, G., Staver, A.C., Aquino, S., Cornelissen, J.H.C., 2013. New handbook for standardised measurement of plant functional traits worldwide. Aust. J. Bot. 61, 167. https://doi.org/10.1071/BT12225.
Pérez-Priego, O., Testi, L., Orgaz, F., Villalobos, F.J., 2010. A large closed canopy chamber for measuring CO2 and water vapour exchange of whole trees. Environ. Exp. Bot. 68 (2), 131–138. https://doi.org/10.1016/j.envexpbot.2009.10.009.
Potts, D.L., Scott, R.L., Cable, J.M., Huxman, T.E., Williams, D.G., 2008. Sensitivity of mesquite shrubland CO2 exchange to precipitation in contrasting landscape settings. Ecology 89, 2900–2910. https://doi.org/10.1890/07-1177.1.
Poulter, B., Frank, D., Ciais, P., Myneni, R.B., Andela, N., Bi, J., Broquet, G., Canadell, J.G., Chevallier, F., Liu, Y.Y., Running, S.W., Sitch, S., van der Werf, G.R., 2014. Contribution of semi-arid ecosystems to interannual variability of the global carbon cycle. Nature 509, 600–603. https://doi.org/10.1038/nature13376.
Prieto, I., Almagro, M., Bastida, F., Querejeta, J.I., 2019. Altered leaf litter quality exacerbates the negative impact of climate change on decomposition. J. Ecol. 107, 2364–2382. https://doi.org/10.1111/1365-2745.13168.
Querejeta, J.I., Ren, W., Prieto, I., 2021. Vertical decoupling of soil nutrients and water under climate warming reduces plant cumulative nutrient uptake, water-use efficiency and productivity. New Phytol. 230, 1378–1393. https://doi.org/10.1111/nph.17258.
R Core Team, 2018. R: a language and environment for statistical computing (version 3.5.2). WebsiteR Foundation for Statistical Computing, Vienna, Austria. http://www.r-project.org.
Rey, A., Carrascal, L.M., Báez, C.G.-G., Raimundo, J., Oyonarte, C., Pegoraro, E., 2021. Impact of climate and land degradation on soil carbon fluxes in dry semiarid grasslands in SE Spain. Plant Soil 461, 323–339. https://doi.org/10.1007/s11104-021-04842-y.
Rey, A., Oyonarte, C., Morán-López, T., Raimundo, J., Pegoraro, E., 2017. Changes in soil moisture predict soil carbon losses upon rewetting in a perennial semiarid steppe in SE Spain. Geoderma 287, 135–146. https://doi.org/10.1016/j.geoderma.2016.06.025.
Rey, A., Pegoraro, E., Oyonarte, C., Were, A., Escribano, P., Raimundo, J., 2011. Impact of land degradation on soil respiration in a steppe (Stipa tenacissima L.) semi-arid ecosystem in the SE of Spain. Soil Biol. Biochem. 43, 393–403. https://doi.org/10.1016/j.soilbio.2010.11.007.
Reynolds, J.F., Smith, D.M.S., Lambin, E.F., Turner, B.L., Mortimore, M., Batterbury, S.P.J., Downing, T.E., Dowlatabadi, H., Fernández, R.J., Herrick, J.E., Huber-Sannwald, E., Jiang, H., Leemans, R., Lynam, T., Maestre, F.T., Ayarza, M., Walker, B., 2007. Global desertification: building a science for dryland development. Science 316, 847–851. https://doi.org/10.1126/science.1131634.

Reynolds, J.F., Virginia, R.A., Kemp, P.R., de Soyza, A.G., Tremmel, D.C., 1999. Impact of drought on desert shrubs: effects of seasonality and degree of resource island development. Ecol. Monogr. 69, 69–106. https://doi.org/10.1890/0012-9615(1999)069[0069:IODODS]2.0.CO;2.

Rouse, J.W., Hass, R.H., Schell, J.A., Deering, D.W., 1974. Proceedings of the Third ERTS Symposium. Vol. I. Monitoring vegetation systems in the Great Plains with ERTS.

Ruiz Sinoga, J.D., Pariente, S., Diaz, A.R., Martinez Murillo, J.F., 2012. Variability of relationships between soil organic carbon and some soil properties in Mediterranean rangelands under different climatic conditions (South of Spain). Catena 94, 17–25. https://doi.org/10.1016/j.catena.2011.06.004.

Salazar-Tortosa, D., Castro, J., Villar-Salvador, P., Viñegla, B., Matías, L., Michelsen, A., Rubio de Casas, R., Querejeta, J.I., 2018. The "isohydric trap": a proposed feedback between water shortage, stomatal regulation, and nutrient acquisition drives differential growth and survival of European pines under climatic dryness. Glob. Chang. Biol. 24, 4069–4083. https://doi.org/10.1111/gcb.14311.

Sánchez-Gómez, P., Carrión, M.A., Hernández, A., Guerra, J., 2003. Libro Rojo de la Flora Silvestre protegida de la región de Murcia. Consejería de Agricultura, Agua y Medio Ambiente, Murcia, Spain.

Schlesinger, W.H., Andrews, J.A., 2000. Soil respiration and the global carbon cycle. Biogeochemistry 48, 7–20. https://doi.org/10.1023/A:1006247623877.

Sommer, B., Froend, R., 2011. Resilience of phreatophytic vegetation to groundwater drawdown: is recovery possible under a drying climate? Ecohydrology 4, 67–82. https://doi.org/10.1002/eco.124.

Sponseller, R.A., 2007. Precipitation pulses and soil CO 2 flux in a Sonoran Desert ecosystem. Glob. Chang.Biol. 13, 426–436. https://doi.org/10.1111/j.1365-2486.2006.01307.x.

Thomey, M.L., Collins, S.L., Vargas, R., Johnson, J.E., Brown, R.F., Natvig, D.O., Friggens, M.T., 2011. Effect of precipitation variability on net primary production and soil respiration in a Chihuahuan Desert grassland: precipitation variability in desert grassland. Glob. Chang.Biol. 17, 1505–1515. https://doi.org/10.1111/j.1365-2486.2010.02363.x.

Tian, F., Brandt, M., Liu, Y.Y., Rasmussen, K., Fensholt, R., 2017. Mapping gains and losses in woody vegetation across global tropical drylands. Glob. Chang.Biol. 23, 1748–1760. https://doi.org/10.1111/gcb.13464.

Tirado, R., 2009. 5220 Matorrales arborescentes con Ziziphus (*). VV.AAaa., Bases ecológicas preliminares para la conservación de los tipos de hábitat de interés comunitario en España. 68. Ministerio de Medio Ambiente. y Medio Rural y Marino.

Torres-García, M.T., Salinas-Bonillo, M.J., Cleverly, J.R., Gisbert, J., Pacheco-Romero, M., Cabello, J., 2021a. A multiple-trait analysis of ecohydrological acclimatisation in a dryland phreatophytic shrub. Oecologia 196, 1179–1193. https://doi.org/10.1007/s00442-021-04993-w.

Torres-García, M.T., Salinas-Bonillo, M.J., Gázquez-Sánchez, F., Fernández-Cortés, Á., Querejeta, J.I., Cabello, J., 2021b. Squandering water in drylands: the water-use strategy of the phreatophyte Ziziphus lotus in a groundwater-dependent ecosystem. Am. J. Bot. 108, 236–248. https://doi.org/10.1002/ajb2.1606.

Torres-García, M.T., Salinas-Bonillo, M.J., Pacheco-Romero, M., Cabello, J., 2021c. Modular growth and functional heterophylly of the phreatophyte Ziziphus lotus: a trait-based study. Plant Species Biol. 1442–1984, 12343. https://doi.org/10.1111/1442-1984.12343.

Tucker, C.L., Reed, S.C., 2016. Low soil moisture during hot periods drives apparent negative temperature sensitivity of soil respiration in a dryland ecosystem: a multi-model comparison. Biogeochemistry 128, 155–169. https://doi.org/10.1007/s10533-016-0200-1.

Vallejos, A., Sola, F., Yechieli, Y., Pulido-Bosch, A., 2018. Influence of the paleogeographic evolution on the groundwater salinity in a coastal aquifer. Cabo de Gata aquifer,SE Spain. J. Hydrol. 557, 55–66. https://doi.org/10.1016/j.jhydrol.2017.12.027.

Vargas, R., Sánchez-Cañete, P.E., Serrano-Ortiz, P., Curiel Yuste, J., Domingo, F., López-Ballesteros, A., Oyonarte, C., 2018. Hot-moments of soil CO2 efflux in a water-limited grassland. Soil Syst. 2, 47. https://doi.org/10.3390/soilsystems2030047.

Wang, X., Ma, Q., Jin, H., Fan, B., Wang, D., Lin, H., 2019. Change in characteristics of soil carbon and nitrogen during the succession of Nitraria tangutorum in an arid desert area. Sustainability 11, 1146. https://doi.org/10.3390/su11041146.

West, A.W., Sparling, G.P., 1986. Modifications to the substrate-induced respiration method to permit measurement of microbial biomass in soils of differing water contents. J. Microbiol. Methods 5, 177–189. https://doi.org/10.1016/0167-7012(86)90012-6.

Whitaker, J., Ostle, N., McNamara, N.P., Nottingham, A.T., Stott, A.W., Bardgett, R.D., Salinas, N., Ccahuana, A.J.Q., Meir, P., 2014. Microbial carbon mineralization in tropical lowland and montane forest soils of Peru. Front. Microbiol. 5. https://doi.org/10.3389/fmicb.2014.00720.

Wu, Z., Dijkstra, P., Koch, G.W., Peñuelas, J., Hungate, B.A., 2011. Responses of terrestrial ecosystems to temperature and precipitation change: a meta-analysis of experimental manipulation: meta-analysis of experimental manipulation. Glob. Chang.Biol. 17, 927–942. https://doi.org/10.1111/j.1365-2486.2010.02302.x.

Zhang, P., Yang, J., Zhao, L., Bao, S., Song, B., 2011. Effect of Caragana tibetica nebkhas on sand entrapment and fertile islands in steppe–desert ecotones on the Inner Mongolia Plateau, China. Plant Soil 347, 79–90. https://doi.org/10.1007/s11104-011-0813-z.

Zolfaghar, S., Villalobos-Vega, R., Cleverly, J., Zeppel, M., Rumman, R., Eamus, D., 2014. The influence of depth-to-groundwater on structure and productivity of Eucalyptus woodlands. Aust. J. Bot. 62, 428. https://doi.org/10.1071/BT14139.